Germanane Monolayer Films as Antibacterial Coatings

Kouloumpis, Antonios; Chatzikonstantinou, Alexandra; Chalmpes, Nikolaos; Giousis, Theodosis; Potsi, Georgia; Katapodis, Petros; Stamatis, Haralambos; Rudolf, Petra

Published in:
ACS Applied Nano Materials

DOI:
10.1021/acsanm.0c03149

Publication date:
2021

ACS APPLIED NANO MATERIALS

www.acsanm.org

Letter

Germanane Monolayer Films as Antibacterial Coatings

Antonios Kouloumpis,* Alexandra V. Chatzikonstantinou, Nikolaos Chalmpes, Theodosis Giousis, Georgia Potsi, Petros Katapodis, Haralambos Stamatis,* Dimitrios Gournis,* and Petra Rudolf*

Cite This: *ACS Appl. Nano Mater.* 2021, 4, 2333−2338

Read Online

ACCESS | Metrics & More | Article Recommendations | Supporting Information

ABSTRACT: Germanane (GeH), a graphane analogue, has attracted significant interest because of its optoelectronic properties; however, the environmental and biological effects of GeH have scarcely been investigated so far. Here we report a facile approach based on the Langmuir−Schaefer deposition to produce homogeneous and dense GeH monolayer films on various substrates. In view of possible applications and to extend the use of GeH to unexplored fields, we investigated its antibacterial activity for the first time and found that this promising 2D structure exhibits remarkable antibacterial activity against both Gram-negative and Gram-positive bacterial strains.

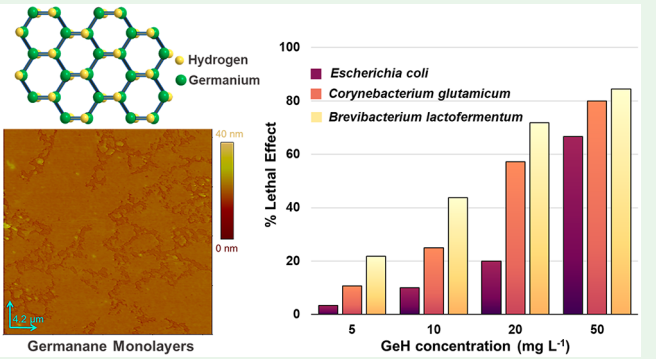

KEYWORDS: *2D materials, germanane, Langmuir−Schaefer deposition, antibacterial coatings, cell membrane rupture, positive surface charge*

The increasing emergence of antibiotic-resistant bacterial strains over the last years urgently calls for the development of new antibacterial drugs or coatings. Significant efforts have focused on the fabrication or improvement of surfaces with antibacterial action—not only for health-related aims but also in view of keeping them clean by preventing the growth of microorganisms. The antibacterial action can be induced by the surface roughness (textile surfaces) as well as by physical or chemical effects[1] and hence achieved by functionalizing, derivatizing, or polymerizing the surfaces.[2] The rapid growth of nanotechnology has opened new routes for thin-film preparation through a diversity of surface modification methods such as plasma and polymerization methods,[3] layer-by-layer assembly,[4] and Langmuir−Blodgett/Schaefer techniques.[5] Despite the multitude of approaches for the formation of antibacterial films, the most common problems still encountered are short-term stability and nonuniformity[6] of the films; additionally, the preparation methods are often not easily transferable to an industrial environment.

Germanane (GeH), the germanium graphane analogue, has attracted considerable interest because of its remarkable combination of properties. The predicted high mobility of GeH and nonzero band gap make it an extremely suitable 2D material for optoelectronic applications,[7] field-effect transistors,[8] and photocatalytic applications.[9] Although these remarkable physicochemical properties of GeH place it in the top group with regard to (opto)electronic devices, its study for bioapplications is still limited. The first promising results concern the potential of germanium-based nanomaterials and compounds in cancer nanomedicine[10] and drug delivery,[11] owing to the antiviral, antimutagenic, antitumor, erythropoietic, and immunomodulating properties of germanium[12] and call for further research of GeH in related applications. In this direction, here we study whether GeH inhibits germ growth and can be promising for the development of antibacterial surfaces.

The production of GeH is based on the substitution of calcium by hydrogen during the topochemical deintercalation of a β-$CaGe_2$-layered Zintl phase in aqueous acids (HCl, HBr, HI, or acetic acid).[13] The reaction is extremely slow and requires between 1 and 2 weeks. Recently, we reported a new synthetic approach for high-purity GeH with aqueous HF at room temperature that allows one to obtain GeH nanocrystals in just a few minutes,[14] as shown in the schematic diagram in Figure 1a.

To study the antibacterial activity, dispersions and coatings of this new Xane were produced. A facile and low-cost Langmuir−Schaefer (LS) deposition was used for obtaining GeH monolayers, with precise control of the packing of the nanosheets in 2D arrays. The LS deposition method consists of spreading molecules or 2D nanosheets at the air−water interface, where they float if hydrophobic or amphiphilic and

Received: November 25, 2020
Accepted: January 29, 2021
Published: February 10, 2021

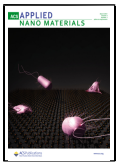

https://dx.doi.org/10.1021/acsanm.0c03149
ACS Appl. Nano Mater. 2021, 4, 2333−2338

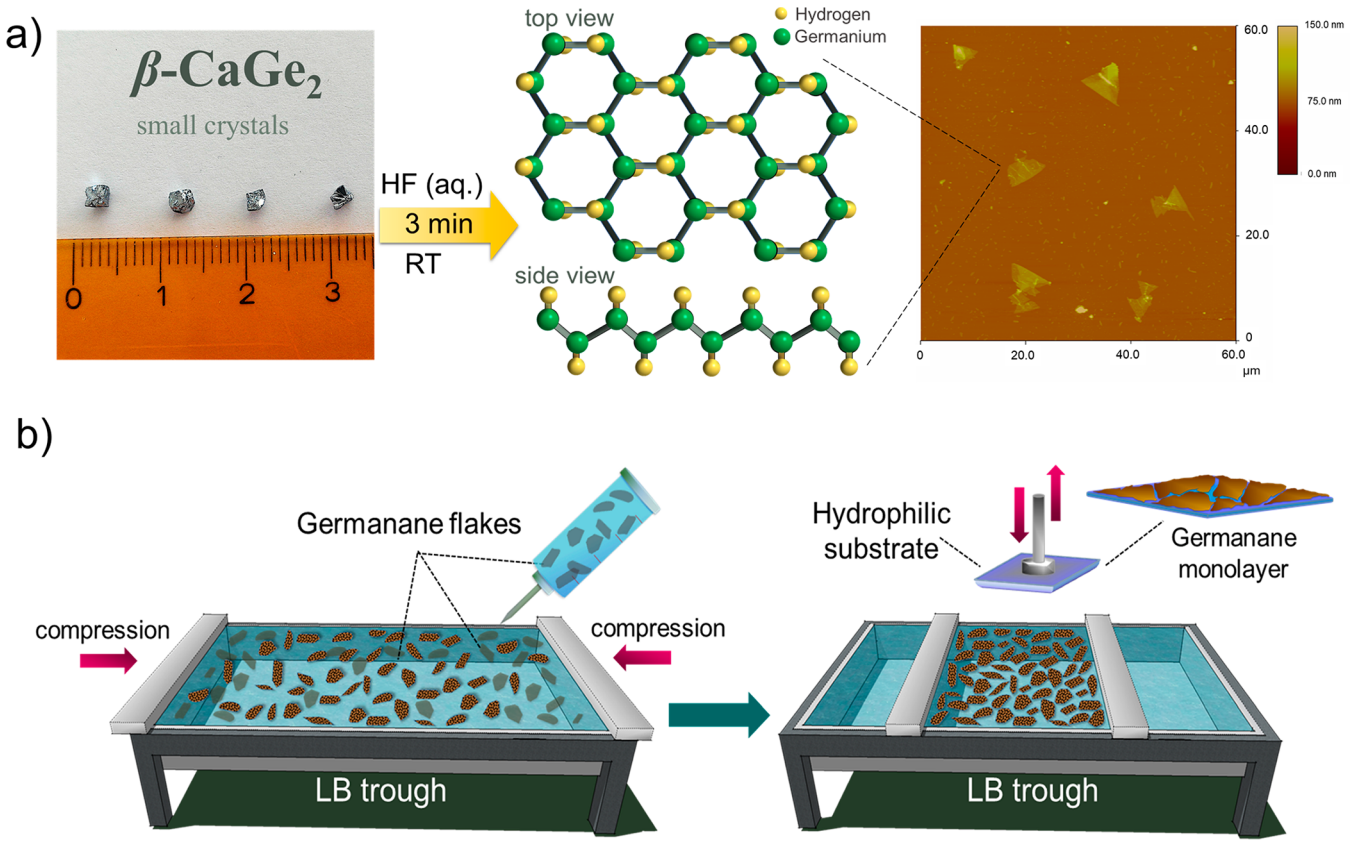

Figure 1. (a) (left) β-$CaGe_2$ Zintl-phase crystals, (middle) GeH structure, and (right) typical AFM height image of GeH flakes. (b) Schematic representation of the LS deposition resulting in GeH monolayers.

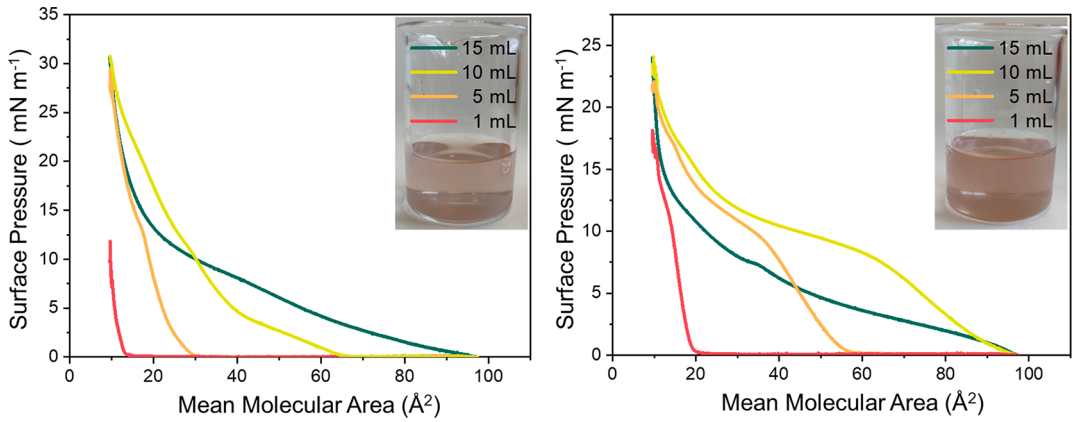

Figure 2. π−A isotherms of floating GeH nanosheets at the water surface for different ethanol (left) and DMF (right) injections ranging from 1 to 15 mL.

can be compressed with the help of two barriers into a densely packed layer called the Langmuir film. This Langmuir film can be transferred to a solid substrate brought into contact by horizontal dipping. GeH is highly dispersible in ethanol and dimethylformamide (DMF) and easily separates into single nanosheets by liquid exfoliation.[15] In addition, droplets of those dispersions can be spread efficiently on a water surface[16] when injected at the air−water interface of the Langmuir−Blodgett trough. Thanks to the hydrophobic nature of GeH (see above), the 2D sheets can be compressed to form a stable floating single-layer film. Uniform monolayers of GeH with high surface coverage were transferred to solid substrates by horizontal dipping of the latter, as shown in Figure 1b.

To show that the GeH used here had the same characteristics as other batches documented in our previous report on the synthesis method,[14] the X-ray diffraction (XRD) pattern as well as the Raman and Fourier transform infrared (FTIR) spectra are reported in Figure S1. To be able to deposit the GeH nanosheets by the LS technique, we first must prove that it is possible to form stable Langmuir films at the water surface. To that end, we recorded π−A isotherms during compression of the Langmuir films formed after different amounts of ethanol dispersions of exfoliated GeH were introduced at the air−water interface. The π−A isotherms for injections ranging from 1 to 15 mL are presented in Figure 2 (left). The curves show a change in the slope when the

https://dx.doi.org/10.1021/acsanm.0c03149
ACS Appl. Nano Mater. 2021, 4, 2333−2338

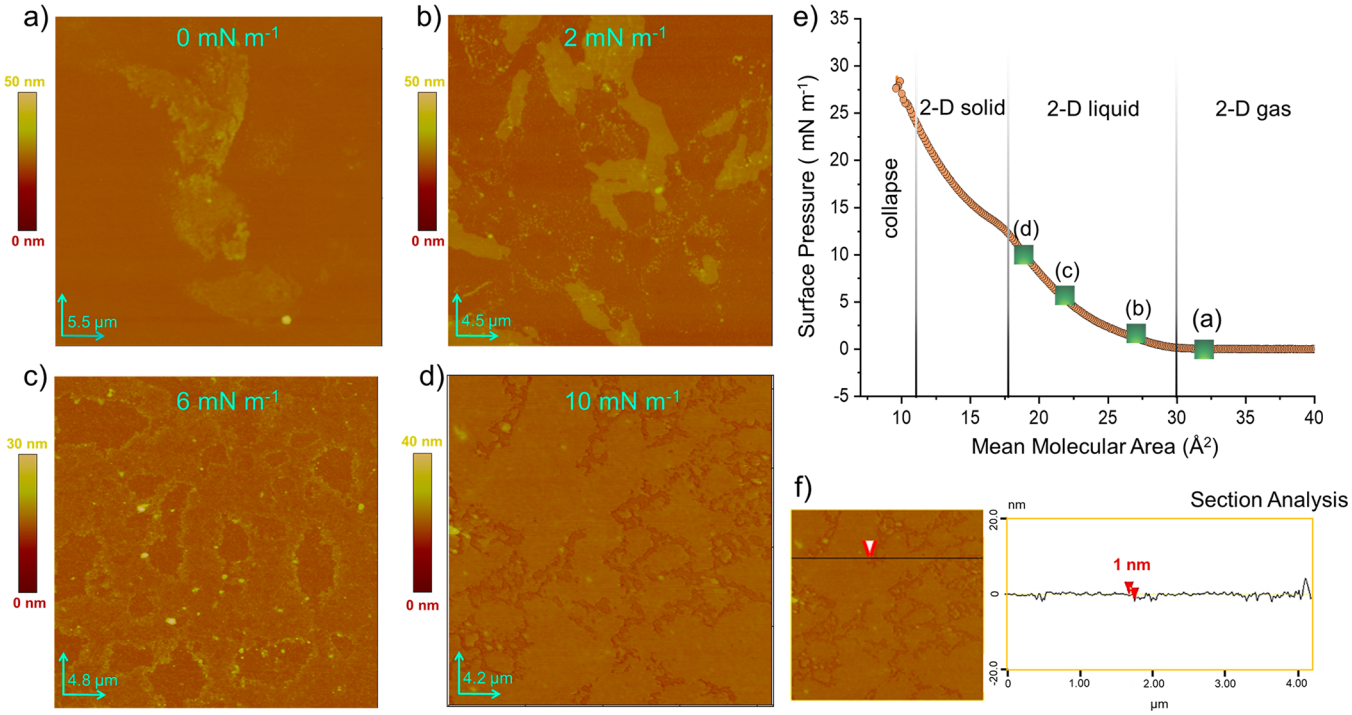

Figure 3. (a–d) AFM height images and (f) cross-sectional analysis of GeH layers on silicon wafers prepared by LS deposition at surface pressures of 0, 2, 6, and 10 mN m^{-1} as recorded from (e) the π–A isotherm from ethanol dispersions (injection of 5 mL).

pressure is such that a phase transition in the Langmuir film of GeH sheets occurs during compression, first from a 2D gas to a 2D liquid and then to a 2D solid.[17] More specifically, following the isotherm from right to left, the first discontinuity is the lift-off area, defined as the molecular area where the surface pressure becomes different from zero; here the flakes start to order and to interact as a 2D liquid. For the π–A isotherm recorded when 1 mL of GeH dispersion was added to the water surface, the lift-off area was 14 $Å^2$ and the maximum surface pressure reached a value of 12 mN m^{-1}.

Phase transitions of the GeH Langmuir films were clearly observed as isotherm slope changes for dispersion volumes of 5 and 10 mL at the water surface, resulting in lift-off areas of 30 and 63 $Å^2$, respectively, while the surface pressure reached a maximum value of 31 mN m^{-1} in both cases. A further increase of the GeH dispersion volume to 15 mL caused an absence of the gas phase and therefore suggests that domains of higher density formed at the water–air interface. Hence, we can conclude that stable Langmuir films are formed, and their density for a certain surface pressure depends on the amount of GeH flakes injected at the water surface.

We also studied the stability of the Langmuir films when GeH flakes are delivered to the water surface in the LB trough in the form of dispersions in DMF. The results for different amounts of dispersion are shown in Figure 2 (right). Similar to that observed for ethanol dispersions, the curves show a change in the slope corresponding to the phase transitions of the Langmuir film of GeH nanosheets during the compression. For 1 mL of GeH dispersion spread on the water surface, the lift-off area was 20 $Å^2$ and the maximum surface pressure reached 18 mN m^{-1}. Phase transitions of the Langmuir film are also clearly observed for a dispersion volume of 5 mL, resulting in a 57 $Å^2$ lift-off area and a surface pressure that reached a maximum value of 24 mN m^{-1}. The absence of a gas phase was observed for larger dispersion volumes of GeH injected at the water surface (10 and 15 mL), suggesting the presence of higher-density domains before compression.

The successful transfer of GeH Langmuir films onto silicon wafers by LS deposition was proven by atomic force microscopy (AFM). Representative AFM height images of the GeH films deposited at different surface pressures are presented in Figure 3a–d. The topographic images show that the surface coverage of the substrate scales with the surface pressure. More specifically, for transfer after the addition of 5 mL of GeH dispersion at the water surface and before compression (at 0 mN m^{-1} surface pressure), single nanosheets with well-defined edges and widely spaced from one another are observed, testifying to the formation of floating layers at the air–water interface (Figure 3a). When the transfer was performed after compression of the floating film to a surface pressure of 2 mN m^{-1}, the LS film consisted of isolated GeH flakes with an empty space between them (Figure 3b).

After transfer at a surface pressure of 6 mN m^{-1}, the GeH nanosheets in the LS film were almost touching, with few voids between them (Figure 3c). Transfer after still further compression of the floating layer to a surface pressure of 10 mN m^{-1} resulted in a closely packed LS film, where the GeH nanosheets formed a homogeneous and dense monolayer that covered ≥80% of the substrate. The average thickness of the GeH flakes as derived from the topographical height profile (Figure 3f) and statistical analysis (Figure S2) was 1.1 ± 0.1 nm, corresponding to a single GeH layer.[14] The micrographs in Figure 3 conclusively prove that LS deposition without the use of a surfactant or stabilizing agent yields homogeneous sparsely or closely packed GeH single layers on solid substrates, identifying this technique as an ideal tool for fabricating thin films of this new 2D material.

The antibacterial activity of GeH dispersions at concentrations between 5 and 50 mg L^{-1} was evaluated using *Escherichia coli* (ECO), *Corynebacterium glutamicum* (COR),

https://dx.doi.org/10.1021/acsanm.0c03149
ACS Appl. Nano Mater. 2021, 4, 2333–2338

and *Brevibacterium lactofermentum* (BRE) as model organisms, as presented in the Supporting Information. As illustrated in Figure 4, overnight exposure of bacteria to an aqueous GeH dispersion at a concentration of 50 mg L^{-1} reduces the bacterial cell population by more than 80% for both Gram-negative and Gram-positive bacterial strains. GeH exhibits a higher lethal effect against Gram-positive bacteria than against Gram-negative ones; probably the more complex cell wall of *E. coli* acts as a barrier toward the antibacterial effect.[18] In all strains, the reduction in the cell population depends on the nanomaterial dosage. The lethal concentration, LC50 (i.e., the concentration of the nanomaterial necessary to reduce the initial bacterial population to 50%, after 20 h of interaction), was calculated as 32 ± 4, 16 ± 2, and 19 ± 3 mg L^{-1} for *E. coli*, *C. glutamicum*, and *B. lactofermentum*, respectively.

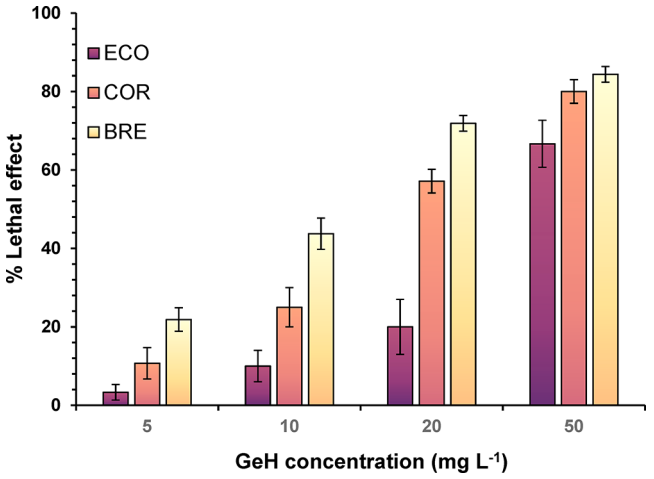

Figure 4. Lethal effect of GeH dispersions against Gram-negative *E. coli* (ECO), Gram-positive *C. glutamicum* (COR), and Gram-positive *B. lactofermentum* (BRE) bacteria. The columns represent the percentages of cell death after overnight interaction. Data are represented as mean ± SD (standard deviation) based on triplicate independent measurements.

Similar results were obtained for GeH monolayers deposited on mylar substrates. The antibacterial activity of GeH thin films was evaluated using the same model organisms, but this time an antibacterial drop-test was used. The lethal effect was determined by measuring the number of remaining live cells after the cells were left on the GeH films overnight.

The bacterial population for all bacterial strains decreased after incubation on the GeH films, as shown in Table 1. The percentage of bacteria remaining viable after exposure scaled with the number of cells applied. When 1.25 × 10^3 CFU cm^{-2} of GeH films were applied, the antibacterial effect was more than 95% for all of the strains. For higher bacterial populations, from 1.25 × 10^4 to 1.25 × 10^5 CFU cm^{-2} of GeH films, the bacterial inhibition of the films was found to depend on the bacterial strain. More specifically, the GeH films exhibited remarkable antibacterial activity against *B. lactofermentum*, and this effect was slightly lower for *C. glutamicum* strains and even weaker for *E. coli*.

Table 1. Lethal Effect of GeH LS Films against Gram-Negative (*E. coli*) and Gram-Positive (*C. glutamicum* and *B. lactofermentum*) Bacteria after Exposure for 20 h

	lethal effect (%) of GeH films with the indicated initial bacteria populations		
bacterial species	1.25 × 10^3 CFU cm^{-2}	1.25 × 10^4 CFU cm^{-2}	1.25 × 10^5 CFU cm^{-2}
E. coli	80 ± 5	70 ± 8	40 ± 5
C. glutamicum	90 ± 5	85 ± 4	70 ± 6
B. lactofermentum	>99	>99	>95

We also observed the morphological changes of *C. glutamicum* before and after contact with GeH by AFM, as shown in Figure S3. *C. glutamicum* on the untreated silicon wafer (Figure S3a,b,e) is typically rod-shaped, and the cell walls appear smooth with no evidence of membrane rupture and collapse. After prolonged contact with GeH, the cell walls appear wrinkled and damaged, which is clear evidence of membrane rupture[19,20] (Figure S3c,d,f).

The observed outstanding antibacterial action of GeH is probably due to physical and chemical processes occurring on germanium-based compounds[21] as well as on other 2D materials such as graphene and its derivatives.[22] The physical factors are related to the "sharp" edges of the nanosheets, cutting through the bacterium's cell membrane and causing the intracellular matrix to leak, which eventually leads to the bacterium's death.[23] From our microscopy studies, we know that the GeH nanosheets deposited on the substrates by the LS method form flat, homogeneous, and closely packed monolayers, with an average roughness of <1 nm, as calculated from AFM analysis (Figure S2, inset), suggesting that the robust antibacterial activity of GeH should not have been observed if the "sharp" edges of the nanosheets were the main cause for rupture of the cell membrane. Another mechanism that has been suggested is self-aggregation or induced aggregation of 2D sheets, which can lead to wrapping or trapping of the bacteria and hence their inactivation, thus inhibiting their proliferation.[24] This mechanism is also not likely because, in our experimental protocol, the bacteria are interacting with GeH layers anchored on a substrate, and such an anchoring prevents aggregation. Because, as shown in Figure S3, the interaction of bacteria with GeH films causes an irreversible lethal effect on the cells, which is similar to that of the GeH sheets in dispersion, we suggest that self-aggregation or induced aggregation cannot be the main reason for the antibacterial effect in the case of the GeH sheets in dispersion either. Moreover, changes in the chemical structure are also unlikely to play a role because the only possible change for GeH is dehydrogenation, and that requires substantial heating.[25] Oxidative stress induced by reactive oxygen species (ROS), which has been proposed to disrupt some microbial processes in the presence of graphene oxide,[19] is not expected here because GeH does not contain oxygen. However, the oxidation of essential cellular components or structure without ROS production, as proposed for fullerene (C_{60}),[26] might occur for GeH, but further investigation is needed to support such a conclusion.

Furthermore, it is worth noting that GeH nanosheets present a water contact angle of 95 ± 3° and a ζ potential of 7.8 mV, as shown in Figure S4; the hydrophobic character and positive surface charge may contribute to interactions with bacterial membrane lipids and cause membrane disruption.[27]

In conclusion, GeH is a new inorganic 2D material with not only outstanding potential for (opto)electronics but also extraordinary antibacterial properties against Gram-negative and Gram-positive bacterial strains both when the latter are exposed to GeH in aqueous dispersion and when they are

https://dx.doi.org/10.1021/acsanm.0c03149
ACS Appl. Nano Mater. 2021, 4, 2333−2338

incubated on GeH thin films. In our work, we achieved an inactivation of more than 80% for both Gram-negative and Gram-positive bacterial strains at a lower concentration (50 μg mL^{-1}) than previous studies of other 2D solids, namely, graphene oxide,[28] MoS_2,[29] and Ti_3C_2Tx (metal carbides/nitrides or MXenes).[30] We also found extraordinary antibacterial activity against the *B. lactofermentum* bacterial strain for all cell concentrations. On the basis of the above results, we are confident in proposing this new material as an attractive antibacterial agent.

■ ASSOCIATED CONTENT

Supporting Information

The Supporting Information is available free of charge at https://pubs.acs.org/doi/10.1021/acsanm.0c03149.

Experimental section, FTIR and Raman spectra and XRD pattern of GeH, AFM analysis of GeH films, AFM images of *C. glutamicum* before and after GeH contact, and ζ potential and water contact angle of GeH (PDF)

■ AUTHOR INFORMATION

Corresponding Authors

Antonios Kouloumpis − *Department of Materials Science & Engineering, University of Ioannina, 45110 Ioannina, Greece; Zernike Institute for Advanced Materials, University of Groningen, 9747 AG Groningen, The Netherlands;* orcid.org/0000-0002-8738-3141; Email: antoniokoul@gmail.com

Haralambos Stamatis − *Biotechnology Laboratory, Department of Biological Applications and Technologies, University of Ioannina, 45110 Ioannina, Greece;* orcid.org/0000-0002-8196-4885; Email: hstamati@uoi.gr

Dimitrios Gournis − *Department of Materials Science & Engineering, University of Ioannina, 45110 Ioannina, Greece;* orcid.org/0000-0003-4256-8190; Email: dgourni@uoi.gr

Petra Rudolf − *Zernike Institute for Advanced Materials, University of Groningen, 9747 AG Groningen, The Netherlands;* orcid.org/0000-0002-4418-1769; Email: p.rudolf@rug.nl

Authors

Alexandra V. Chatzikonstantinou − *Biotechnology Laboratory, Department of Biological Applications and Technologies, University of Ioannina, 45110 Ioannina, Greece*

Nikolaos Chalmpes − *Department of Materials Science & Engineering, University of Ioannina, 45110 Ioannina, Greece*

Theodosis Giousis − *Department of Materials Science & Engineering, University of Ioannina, 45110 Ioannina, Greece; Zernike Institute for Advanced Materials, University of Groningen, 9747 AG Groningen, The Netherlands*

Georgia Potsi − *Department of Materials Science & Engineering, University of Ioannina, 45110 Ioannina, Greece; Zernike Institute for Advanced Materials, University of Groningen, 9747 AG Groningen, The Netherlands*

Petros Katapodis − *Biotechnology Laboratory, Department of Biological Applications and Technologies, University of Ioannina, 45110 Ioannina, Greece*

Complete contact information is available at: https://pubs.acs.org/10.1021/acsanm.0c03149

Author Contributions

A.K., H.S., D.G., and P.R. conceived the project, A.K., N.C., T.G., and G.P. synthesized and characterized the GeH samples, and A.V.C., P.K., and H.S. studied the antibacterial activity. The manuscript was written with contributions of all authors. All authors have given approval to the final version of the manuscript.

Notes

The authors declare no competing financial interest.

■ ACKNOWLEDGMENTS

This work received support from the project "National Infrastructure in Nanotechnology, Advanced Materials and Micro-/Nanoelectronics" (MIS-5002772), implemented under the action "Reinforcement of the Research and Innovation Infrastructure", funded by the Operational Programme "Competitiveness, Entrepreneurship and Innovation" (NSRF 2014-2020), and cofinanced by Greece and the European Union (European Regional Development Fund). N.C. gratefully acknowledges the IKY foundation for financial support. This research was also cofinanced by Greece and the European Union (European Social Fund) through the Operational Programme "Human Resources Development, Education and Lifelong Learning" in the context of the project "Strengthening Human Resources Research Potential via Doctorate Research" (MIS-5000432), implemented by the State Scholarships Foundation (IKY). Additional support came from the "Top Research School" programme of the Zernike Institute for Advanced Materials under the Bonus Incentive Scheme of The Netherlands' Ministry of Education, Science, and Culture.

■ REFERENCES

(1) Rigo, S.; Cai, C.; Gunkel-Grabole, G.; Maurizi, L.; Zhang, X.; Xu, J.; Palivan, C. G. Nanoscience-Based Strategies to Engineer Antimicrobial Surfaces. *Advanced Science* **2018**, *5* (5), 1700892.

(2) Wang, L.; Hu, C.; Shao, L. The Antimicrobial Activity of Nanoparticles: Present Situation and Prospects for the Future. *Int. J. Nanomed.* **2017**, *12*, 1227−1249.

(3) Nikiforov, A.; Deng, X.; Xiong, Q.; Cvelbar, U.; Degeyter, N.; Morent, R.; Leys, C. Non-Thermal Plasma Technology for the Development of Antimicrobial Surfaces: A Review. *J. Phys. D: Appl. Phys.* **2016**, *49* (20), 204002.

(4) Zhu, X.; Jun Loh, X. Layer-by-Layer Assemblies for Antibacterial Applications. *Biomater. Sci.* **2015**, *3* (12), 1505−1518.

(5) Mangadlao, J. D.; Santos, C. M.; Felipe, M. J. L.; De Leon, A. C. C.; Rodrigues, D. F.; Advincula, R. C. On the Antibacterial Mechanism of Graphene Oxide (GO) Langmuir-Blodgett Films. *Chem. Commun.* **2015**, *51* (14), 2886−2889.

(6) Ajaev, V. S.; Gatapova, E. Y.; Kabov, O. A. Stability and Break-up of Thin Liquid Films on Patterned and Structured Surfaces. *Adv. Colloid Interface Sci.* **2016**, *228*, 92−104.

(7) Liu, N.; Qiao, H.; Xu, K.; Xi, Y.; Ren, L.; Cheng, N.; Cui, D.; Qi, X.; Xu, X.; Hao, W.; Dou, S. X.; Du, Y. Hydrogen Terminated Germanene for a Robust Self-Powered Flexible Photoelectrochemical Photodetector. *Small* **2020**, *16* (23), 2000283.

(8) Madhushankar, B. N.; Kaverzin, A.; Giousis, T.; Potsi, G.; Gournis, D.; Rudolf, P.; Blake, G. R.; Van Der Wal, C. H.; Van Wees, B. J. Electronic Properties of Germanane Field-Effect Transistors. *2D Mater.* **2017**, *4* (2), 021009.

(9) Liu, Z.; Lou, Z.; Li, Z.; Wang, G.; Wang, Z.; Liu, Y.; Huang, B.; Xia, S.; Qin, X.; Zhang, X.; Dai, Y. GeH: A Novel Material as a Visible-Light Driven Photocatalyst for Hydrogen Evolution. *Chem. Commun.* **2014**, *50* (75), 11046−11048.

(10) Ouyang, J.; Feng, C.; Ji, X.; Li, L.; Gutti, H. K.; Kim, N. Y.; Artzi, D.; Xie, A.; Kong, N.; Liu, Y. N.; Tearney, G. J.; Sui, X.; Tao,

W.; Farokhzad, O. C. 2D Monoelemental Germanene Quantum Dots: Synthesis as Robust Photothermal Agents for Photonic Cancer Nanomedicine. *Angew. Chem., Int. Ed.* **2019**, *58* (38), 13405−13410.
(11) Feng, C.; Ouyang, J.; Tang, Z.; Kong, N.; Liu, Y.; Fu, L. Y.; Ji, X.; Xie, T.; Farokhzad, O. C.; Tao, W. Germanene-Based Theranostic Materials for Surgical Adjuvant Treatment: Inhibiting Tumor Recurrence and Wound Infection. *Matter* **2020**, *3* (1), 127−144.
(12) Li, L.; Ruan, T.; Lyu, Y.; Wu, B. Advances in Effect of Germanium or Germanium Compounds on Animals—A Review. *J. Biosci. Med.* **2017**, *05* (07), 56−73.
(13) Jiang, S.; Bianco, E.; Goldberger, J. E. The Structure and Amorphization of Germanane. *J. Mater. Chem. C* **2014**, *2* (17), 3185−3188.
(14) Giousis, T.; Potsi, G.; Kouloumpis, A.; Spyrou, K.; Georgantas, Y.; Chalmpes, N.; Dimos, K.; Antoniou, M. K.; Papavassiliou, G.; Bourlinos, A. B.; Kim, H. J.; Wadi, V. K. S.; Alhassan, S.; Ahmadi, M.; Kooi, B. J.; Blake, G.; Balazs, D. M.; Loi, M. A.; Gournis, D.; Rudolf, P. Synthesis of 2D Germanane (GeH): A New, Fast, and Facile Approach. *Angew. Chem., Int. Ed.* **2021**, *60* (1), 360−365.
(15) Nakamura, D.; Nakano, H. Liquid-Phase Exfoliation of Germanane Based on Hansen Solubility Parameters. *Chem. Mater.* **2018**, *30* (15), 5333−5338.
(16) Large, M. J.; Ogilvie, S. P.; King, A. A. K.; Dalton, A. B. Understanding Solvent Spreading for Langmuir Deposition of Nanomaterial Films: A Hansen Solubility Parameter Approach. *Langmuir* **2017**, *33* (51), 14766−14771.
(17) Zhang, Y.; Xu, L.; Walker, W. R.; Tittle, C. M.; Backhouse, C. J.; Pope, M. A. Langmuir Films and Uniform, Large Area, Transparent Coatings of Chemically Exfoliated MoS2 Single Layers. *J. Mater. Chem. C* **2017**, *5* (43), 11275−11287.
(18) Epand, R. M.; Epand, R. F. Lipid Domains in Bacterial Membranes and the Action of Antimicrobial Agents. *Biochim. Biophys. Acta, Biomembr.* **2009**, *1788* (1), 289−294.
(19) Liu, S.; Zeng, T. H.; Hofmann, M.; Burcombe, E.; Wei, J.; Jiang, R.; Kong, J.; Chen, Y. Antibacterial Activity of Graphite, Graphite Oxide, Graphene Oxide, and Reduced Graphene Oxide: Membrane and Oxidative Stress. *ACS Nano* **2011**, *5* (9), 6971−6980.
(20) Matharu, R. K.; Tabish, T. A.; Trakoolwilaiwan, T.; Mansfield, J.; Moger, J.; Wu, T.; Lourenço, C.; Chen, B.; Ciric, L.; Parkin, I. P.; Edirisinghe, M. Microstructure and Antibacterial Efficacy of Graphene Oxide Nanocomposite Fibres. *J. Colloid Interface Sci.* **2020**, *571*, 239−252.
(21) Al, Q. K.; Bassam, O. A.; Milton, W. Antibacterial Effects of Pure Metals on Clinically Important Bacteria Growing in Planktonic Cultures and Biofilms. *Afr. J. Microbiol. Res.* **2014**, *8* (10), 1080−1088.
(22) Kurapati, R.; Kostarelos, K.; Prato, M.; Bianco, A. Biomedical Uses for 2D Materials Beyond Graphene: Current Advances and Challenges Ahead. *Adv. Mater. (Weinheim, Ger.)* **2016**, *28* (29), 6052−6074.
(23) Kaur, J.; Singh, M.; Dell'Aversana, C.; Benedetti, R.; Giardina, P.; Rossi, M.; Valadan, M.; Vergara, A.; Cutarelli, A.; Montone, A. M. I.; Altucci, L.; Corrado, F.; Nebbioso, A.; Altucci, C. Biological Interactions of Biocompatible and Water-Dispersed MoS2 Nanosheets with Bacteria and Human Cells. *Sci. Rep.* **2018**, *8* (1). DOI: 10.1038/s41598-018-34679-y.
(24) Akhavan, O.; Ghaderi, E.; Esfandiar, A. Wrapping Bacteria by Graphene Nanosheets for Isolation from Environment, Reactivation by Sonication, and Inactivation by near-Infrared Irradiation. *J. Phys. Chem. B* **2011**, *115* (19), 6279−6288.
(25) Chen, Q.; Liang, L.; Potsi, G.; Wan, P.; Lu, J.; Giousis, T.; Thomou, E.; Gournis, D.; Rudolf, P.; Ye, J. Highly Conductive Metallic State and Strong Spin-Orbit Interaction in Annealed Germanane. *Nano Lett.* **2019**, *19* (3), 1520−1526.
(26) Lyon, D. Y.; Brunet, L.; Hinkal, G. W.; Wiesner, M. R.; Alvarez, P. J. J. Antibacterial Activity of Fullerene Water Suspensions (NC 60) Is Not Due to ROS-Mediated Damage. *Nano Lett.* **2008**, *8* (5), 1539−1543.
(27) Asri, L. A. T. W.; Crismaru, M.; Roest, S.; Chen, Y.; Ivashenko, O.; Rudolf, P.; Tiller, J. C.; Van Der Mei, H. C.; Loontjens, T. J. A.; Busscher, H. J. A Shape-Adaptive, Antibacterial-Coating of Immobilized Quaternary-Ammonium Compounds Tethered on Hyperbranched Polyurea and Its Mechanism of Action. *Adv. Funct. Mater.* **2014**, *24* (3), 346−355.
(28) Hu, W.; Peng, C.; Luo, W.; Lv, M.; Li, X.; Li, D.; Huang, Q.; Fan, C. Graphene-Based Antibacterial Paper. *ACS Nano* **2010**, *4* (7), 4317−4323.
(29) Yang, X.; Li, J.; Liang, T.; Ma, C.; Zhang, Y.; Chen, H.; Hanagata, N.; Su, H.; Xu, M. Antibacterial Activity of Two-Dimensional MoS2 Sheets. *Nanoscale* **2014**, *6* (17), 10126−10133.
(30) Rasool, K.; Helal, M.; Ali, A.; Ren, C. E.; Gogotsi, Y.; Mahmoud, K. A. Antibacterial Activity of Ti3C2Tx MXene. *ACS Nano* **2016**, *10* (3), 3674−3684.

https://dx.doi.org/10.1021/acsanm.0c03149
ACS Appl. Nano Mater. 2021, 4, 2333−2338